$Cu_2ZnSnSe_4$: How far does off-stoichiometry go?

G. Gurieva[1], R. Ferreira[1,2], P. Knoll[3] and S. Schorr[1,3]*

[1] Helmholtz Zentrum Berlin für Materialien und Energie GmbH, Hahn-Meitner-Platz 1, D-14109 Berlin, Germany
[2] Universidade de Coimbra, Physics Department, Rua Larga, 3004-516, Coimbra, Portugal
[3] Freie Universitaet Berlin, Institute of Geological Sciences, Malteserstr. 74-100, Berlin, Germany

E-mail: galina.gurieva@helmholtz-berlin.de

Polycrystalline powder samples of eight very far off-stoichiometric $Cu_2ZnSnSe_4$ (CZTSe) compounds (off-stoichiometry types A - D) are grown using the solid-state reaction method in evacuated silica tubes. An additional thermal annealing is performed, in order to study the influence of annealing on the phase content and stoichiometry of the CZTSe phases formed under these conditions. The structural characterization of the synthesized materials before as well as after annealing is carried out by powder X-ray diffraction (PXRD), paying a special attention to the possibility of minimization the content of secondary phases. Wavelength dispersive X-ray spectroscopy (WDX) is used to determine the chemical composition of the obtained phases, paying a special attention to the phase constituents as well as the evolution of the CZTSe phases after the additional annealing. A comparative study of the phase content of very far off-stoichiometric CZTSe compounds is presented. The possible limits of the existence region of the kesterite CZTSe are discussed.

1. Introduction

Quaternary $Cu_2ZnSnSe_4$ (CZTSe) is a promising low cost, environmentally friendly semiconductor material for absorber layers in thin film solar cells due to a number of advantageous properties it possesses[1]. First of all it consists only of non-toxic or low toxic elements, direct band gap around 1 eV and high absorption coefficient ($> 10^4\,cm^{-1}$) are the next on the list of the advantages of this material [2-4] as well as p-type conductivity [5] and very flexible kesterite type structure [6]. Nevertheless, a common phenomenon observed in CZTSe - based photovoltaic devices is a low open circuit voltage with respect to the band gap, evidencing the existence of a number of challenges that must still be faced in order to achieve high quality, efficient solar cells. A plausible reason for this phenomenon could be the reduction in the effective band gap due to inhomogeneities in structure, phase, or composition. The highest conversion efficiency of CZTSe solar cells is above 11%, where the absorber layer of the device exhibits an off-stoichiometric, copper poor zinc rich composition [7]. Stoichiometry deviations lead to the formation of intrinsic point defects, which significantly influence the electrical and optical properties of the material [8]. The existence of off-stoichiometric single phase CZTSe as well as intrinsic point defects belonging to different off-stoichiometry types was studied recently [9, 10], showing a relatively small region of existence of single phase CZTSe, while the limits of the co-existence of kesterite and secondary phases haven't been reached yet. Another study performed on thin films using synchrotron radiation, dealing with the discrepancy between integral and local composition have introduced some extremely off-stoichiometric compositions [11]. Therefore, a further study of strong deviations from stoichiometry and the existence region of the kesterite type phase is of great importance for the understanding of device performances.

This work is focused on the investigation of the potential limits to the existence of the kesterite, aiming at synthesizing very far off-stoichiometric CZTSe according to the A-D off-stoichiometry types.

2. Experimental

In order to evaluate the possible limits of far off-stoichiometric CZTSe (A-D off-stoichiometry types [9,10,12,13], with A and B types corresponding to the Cu poor/Zn rich compositions and C and D to Cu rich/Zn poor compositions), 8 very far off-stoichiometric samples were prepared via solid-state reaction of pure elements. For each of the samples a mixture of copper (5N), zinc (5N), tin (5N) and selenium (4N) weighted in the calculated composition, were placed in a pyrolytic graphite boat and sealed in an evacuated quartz ampoule. The tubes were placed in a one-zone furnace and heated with 10 K/h in 3 steps (250°C and 450°C) up to 750°C. After holding the final temperature for 240 h the samples were cooled to room temperature in the regime of "switched off furnace". A homogenization step (grinding in an agate mortar and pressing pellets) was followed by annealing the pellets in evacuated silica tubes in the one-zone furnace at an annealing temperature of 750°C for 240 h, followed by a natural cooling. For each of the types, two far off-stoichiometry samples were aimed for, with the intended Cu/(Zn+Sn) and Zn/Sn ratios being chose equal to 0.5 and 1.5 in the attempt to reach the existence limits of CZTSe in these directions. The full list of the investigated compositions is presented in **Table 1.** The analysis of the samples after the above-mentioned procedure showed them to be extremely heterogeneous, so an attempt at minimizing the number of secondary phases and perhaps reducing the number of kesterite phases to a single one by means of a second thermal annealing (the same procedure as the first one) was implemented.

In order to determine the chemical composition of the eight powder samples, wavelength dispersive X-ray spectroscopy (WDX) has been applied using an electron microprobe analysis system. **Figure 1** presents the backscatter electron (BSE) micrographs showing the inhomogeneity of the CZTSe samples. To gain reliable results from the WDX measurements, the system was calibrated using elemental standards. High accuracy of the compositional parameters was achieved by averaging over 20 local measurement points within one grain and paying special attention to the search of the secondary phases. For the kesterite phases at least

50 grains were measured for each sample, in this way producing a reliable figure of kesterite phase compositions distribution in each of the samples. This type of analysis was applied twice – after the first annealing and after the second thermal annealing, in this way providing valuable information about the changes in the phase content of the corresponding samples as well as information on the changes in the kesterite phases of the samples with annealing, within the resolution of the WDX.

Powder X-ray diffraction data of all eight samples at both stages (after the first and after the second annealing) were collected at room temperature using a PANalytical X'pertPro MPD diffractometer equipped with CuKα radiation (λ=1.54056 Å) in a focusing Bragg-Brentano geometry. Unfortunately, due to the presence of multiple kesterite phases in the samples – which are almost impossible to resolve, Rietveld refinement of the obtained diffraction data wasn't performed. Only phase analysis using the Powdercell [14] software was applied, allowing us to qualitatively analyze the phase content and changes in the diffraction patterns before and after the second annealing.

3. Results and discussion

All of the obtained samples showed quarternary phases to be prevalent, but the presence of different secondary phases in different regions of the cation ratio plot was found. The cation ratios of the kesterite type phases resulting from the electron microprobe analysis for each of the four aimed types are plotted in **Figure 2**. The cation ratio plot Cu/(Zn+Sn) vs. Zn/Sn gives a better overview of a quaternary system like CZTSe because here two ratios have to be considered to define the chemical composition. Both cation ratios equal to one corresponding to a stoichiometric kesterite. The lines correspond to the different off-stoichiometry types (A - L) [9] and have been calculated accordingly. According to the cation ratios, the synthesized off-stoichiometric kesterites aimed as A-type, B-type, C-type and D-type turned out to be mostly mixtures of two types, which is the result of the presence of more than one kesterite phase with different compositions as well as the formation of secondary phases. A complete list of the

obtained kesterite phases and the information on the secondary phases content for all of the samples are presented in **Table 2**.

The combined results from the XRD and WDX investigation of the A-type samples, agree on the presence of the two secondary phases - ZnSe and $SnSe_2$ in both samples **Figure 3**. The kesterite composition even though is far from the intended still falls in the Cu poor, Zn rich region. After the additional annealing, no significant changes in the presence of the secondary phases were detected, while the composition of the kesterite phase was shifted towards the A-type line in both of the cases Figure 2. Results from the B-type samples identify the presence of the ZnSe secondary phase in both samples (Table 2, Figure 2 and 3), before and after annealing, which is in a good agreement with previously reported [9,10]. As shown in Figure 2, the number of kesterite phases found in sample B-001 increased to three compositions from the previous two after the second annealing, as well as in the case of sample B-002. Two of the phase's compositions in B-001 has seemingly only increased in the value of the Zn/Sn ratio, shifting closer to the B-type line from the two previous compositions found. However, the third phase's composition is found in a more Cu-poor region with a lower Cu/(Zn+Sn) ratio than that of the planned composition and a Zn/Sn ratio in between the two previous ones. Kesterite phase compositions in sample B-002 have shifted to a significantly lower Cu/(Zn+Sn) ratio region, though the Zn/Sn ratios have mostly stayed at the same level. Investigation of the C-type samples revealed that grains of Cu_2SnSe_3 and $SnSe_2$ secondary phases were found, confirming the findings of the study with X-ray diffraction. Still, the presence of Cu_2Se was also determined in sample C-002. Lack of success in identifying the presence of this phase in the sample's diffraction pattern could be explained by the complete overlap of its peaks by those of Cu_2SnSe_3, which would be hard to notice in a basic analysis with the PowderCell software. Two distinct kesterite phases were measured in each C-type sample. Compositions of these phases in sample C-001 seem to have shifted from those of the first annealing by an increase of the Cu/(Zn+Sn) ratios and a decrease of the Zn/Sn ratios, with one of the phases almost reaching

the planned composition. The D-type fraction of the measured phases has also increased, as seen in Figure 2. Kesterite phase compositions of sample C-002 follow the opposite trend by concentrating in lower Cu/(Zn+Sn) ratios than those from the first annealing. Furthermore, D-type fractions of these phases have decreased since the compositions are closer to the C-type off-stoichiometry line. Secondary phases detected by WDX measurements of the D-type samples are in agreement with the contents determined by the structural study and results are presented in Table 2. In sample D-001, only Cu_2Se was found, while in sample D-002, both Cu_2Se and Cu_2SnSe_3 were found. Similarly to the C-type samples, the number of distinct kesterite phases in the D-type samples have remained the same, with each sample containing two different compositions. Comparably to the changes seen in sample C-002, phase compositions in sample D-001 are concentrated in lower Cu/(Zn+Sn) ratios and become closer to the D-type line with the second annealing, lowering the C-type fraction of these kesterite phases. Changes in the phase compositions of sample D-002 are almost identical to the ones observed in sample C-001. The same shift in relation to the ratios of the first annealing, causing compositions to become more Cu-rich and slightly more Zn-poor, is easily observed by comparing these samples in Figure 2. Again, the D-type fraction of the determined compositions increased as they have shifted towards the corresponding off-stoichiometry type line.

WDX in combination with the XRD data analysis results confirms that the qualitative phase contents of the entire set of samples are not suffering drastic changes during the second annealing, as well as the secondary phase content is in a reasonably good agreement with the previous findings [9,10]. Regarding the composition of the kesterite phases, none of the intended compositions were reached, most probably due to the formation of the secondary phases. A few far off-stoichiometric kesterite compositions were found to be present in the synthesized samples, but unfortunately, in all of the cases, more than one kesterite composition was observed. The additional annealing, aimed at the reduction or concentration of the kesterite

phase compositions failed. Moreover, the opposite of the intended outcome occurred and, instead of reducing the diversity of CZTSe compositions in each sample, the number actually increased in some or remained identical. The compositions themselves have shown a shift from the previous cation ratios as well, but these are not similar enough across samples to identify the exact effects of the re-annealing in general parameters, though some compositions appear to shift in the direction of off-stoichiometry lines. Even though this process was unable to improve the homogeneity of the samples, results do appear to show potential limits to the existence of the kesterite phase, since none of the compositions measured have crossed outside the boundaries shown in **Figure 4**.

4. Conclusions

Polycrystalline powder samples of eight very far off-stoichiometric $Cu_2ZnSnSe_4$ (CZTSe) compounds were grown using the solid state reaction method. The chemical analysis and structural characterization of the synthesized materials before as well as after additional annealing paying a special attention to the secondary phases content was carried out. The structural study concluded that the additional annealing had no strong influence on the type and amount of the present secondary phases. While it was hard to conclude on the changes in the kesterite phase from the structural characterisation, according to the results of the WDX measurements, the CZTSe phases were altered significantly duting the annealing process. A shift in direction of off-stoichiometry type – lines in case of A and B type samples was observed, while the shift to less off-stoichiometric compositions in case of C and D type samples was discovered. Results of the WDX measurements appear to show potential limits to the existence of the kesterite phase since none of the compositions measured have crossed outside the boundaries of Cu/(Zn+Sn)= 0.6-1.7, Zn/Sn=0.5-1.6 within the resolution of the WDX method.

References

[1]   S. Siebentritt, S. Schorr, *Prog. Photovoltaics: Res. Appl.*, **2012**, *20(5)*, 512.

[2]   M. Leon, S. Levcenko, R. Serna, I. V. Bodnar, A. Nateprov, M. Guc, G.Gurieva, N. Lopez, J. M. Merino, R. Caballero, S. Schorr, A. Perez-Rodriguez, E. Arushanov, *Appl. Phys. Lett.*, **2014**, *105(6)*, 061909.

[3]   S. J. Ahn, S. Jung, J. Gwak, A. Cho, K. Shin, K. Yoon, D. Park, H.Cheong, J. H. Yun, *Appl. Phys. Lett*., **2010,** *97(2)*, 021905.

[4]   L. Gütay, A. Redinger, R. Djemour, S. Siebentritt, *Appl. Phys. Lett.*, **2012**, *100(10)*, 102113.

[5]   R. Adhi Wibowo, E. Soo Lee, B. Munir, and K. Ho Kim, *Phys. Status Solidi A*, **2007**, *204(10)*, 3373.

[6]   S. Schorr, *Sol. Energy Mater. Sol. Cells*, **2011**, *95(6)*, 1482.

[7]   Y. S. Lee, T. Gershon, O. Gunawan, T. K. Todorov, T. Gokmen, Y.Virgus, and S. Guh, *Adv. Energy Mater.*, **2015**, *5(7)*, 1401372.

[8]   S. Chen, A. Walsh, X.-G. Gong, S.-H. Wei, *Adv. Mater.* **2013,** *25(11)*, 1522.

[9]   L. E. Valle Rios, K. Neldner, G. Gurieva, S. Schorr, *J Alloys Compd.* **2016**, *657*, 408.

[10]   G. Gurieva, L. E. Valle Rios, A. Franz, P. Whitfield, S. Schorr, *J. Appl. Phys.,* **2018**, *123*, 161519.

[11]   P. Schöple, G. Gurieva, S. Giraldo, G. Martinez-Criado, C. Ronning, E.Saucedo, S. Schorr, C. S. Schnohr, *Appl. Phys. Lett.*. **2017**, *110*, 043901.

[12]   A. Lafond, L. Choubrac, C. Guillot-Deudon, P. Deniard, and S. Jobic, Z.*Anorg. Allg. Chem*., **2012**, *638(15)*, 2571.

[13]   G. Gurieva, S. Levcenco, A. Pereira Correia de Sousa, T. Unold, S. Schorr, *Phys. Status Solidi C*, **2017**, 1700166.

[14]   W. Kraus, G. Nolze, *J. Appl. Cryst.*, **1996**, *29*, 301-303.

Figure 1. Backscattered electron micrographs of a) A-002 sample, $SnSe_2$ detected in white grains and ZnSe as a darker gray; b) D-002 sample displaying a dark grey grain where Cu_2SnSe_3 and light grey Cu_2Se were found.
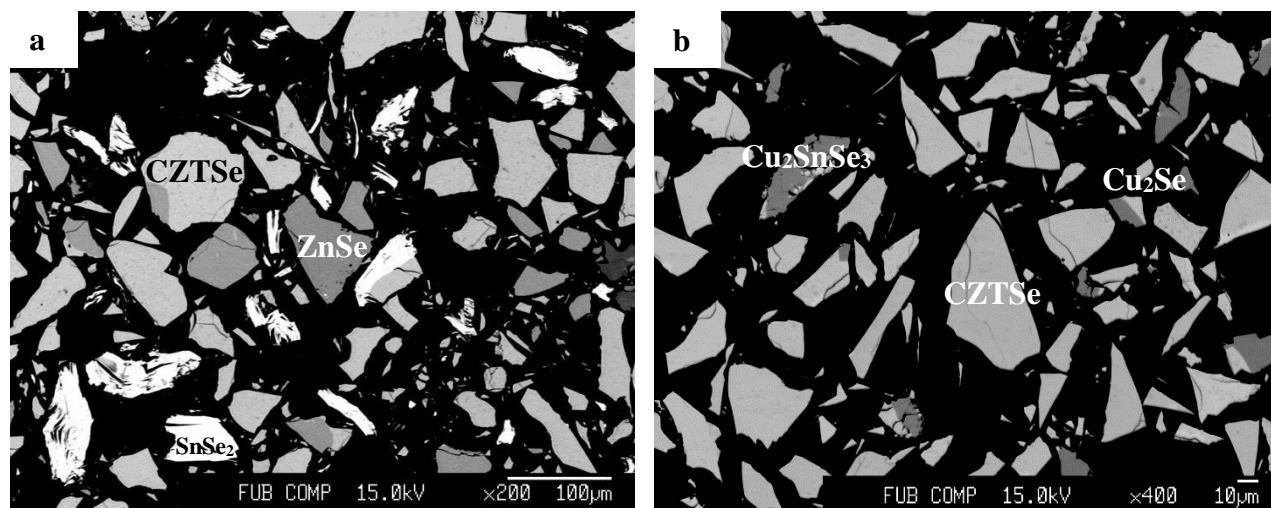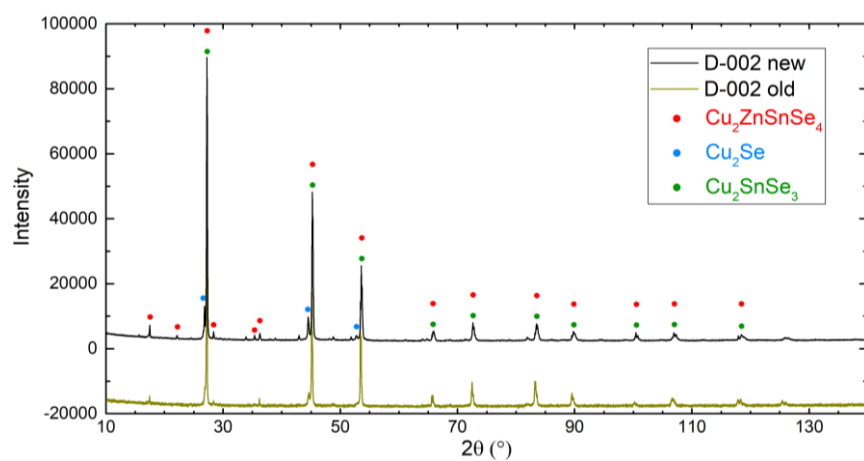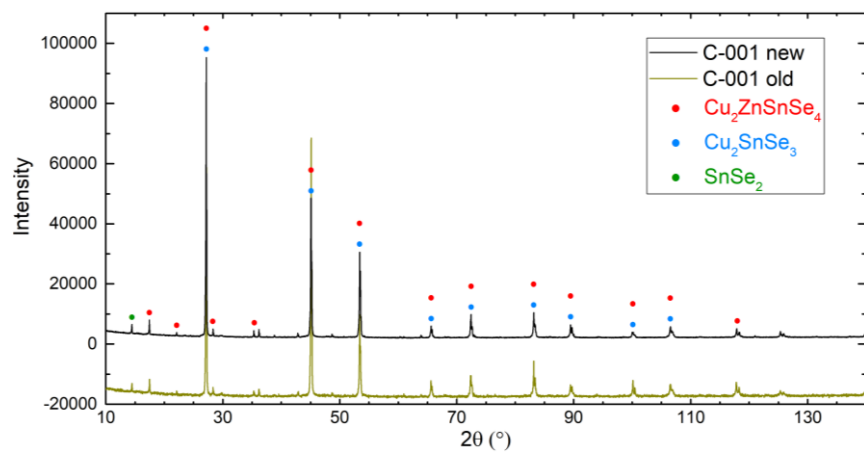
Figure 2. Cation Ratio plots for A-001, A-002, B-001, B-002, C-001, C-002, D-001 and D-002 samples.
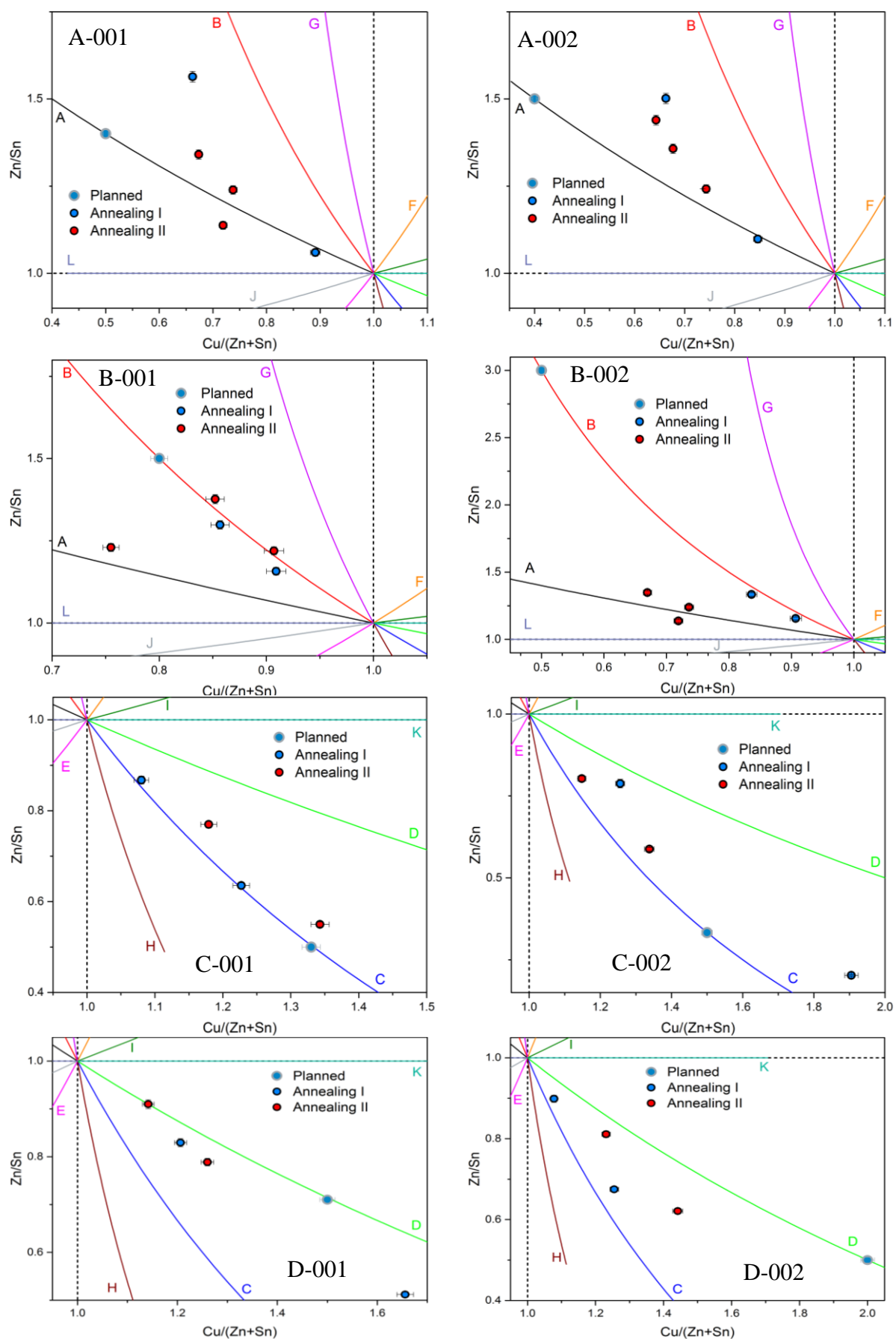
Figure 3. Diffraction patterns from samples A-002, B-002, C-001 and D-002, with color-coded diffraction peaks from secondary phases.
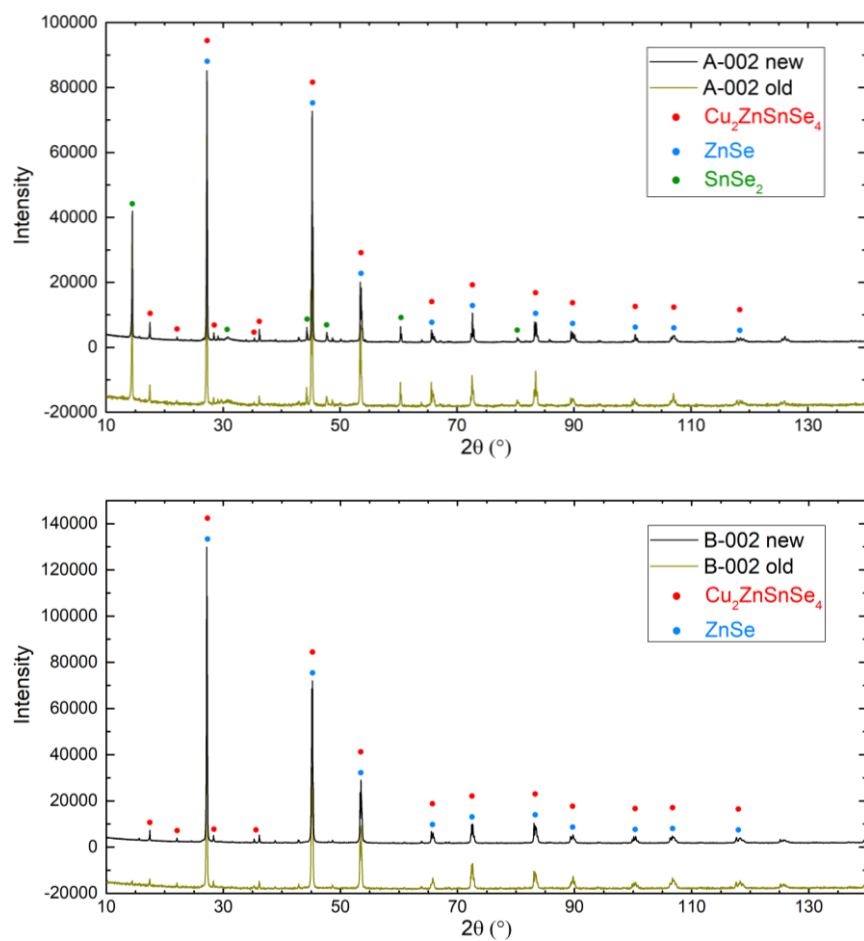
Figure 4. Complete set of results from WDX measurements, of the 8 far off-stoichiometric CZTSe samples showing all the kesterite compositions measured and possible existence limits of this phase within the resolution limits of WDX.
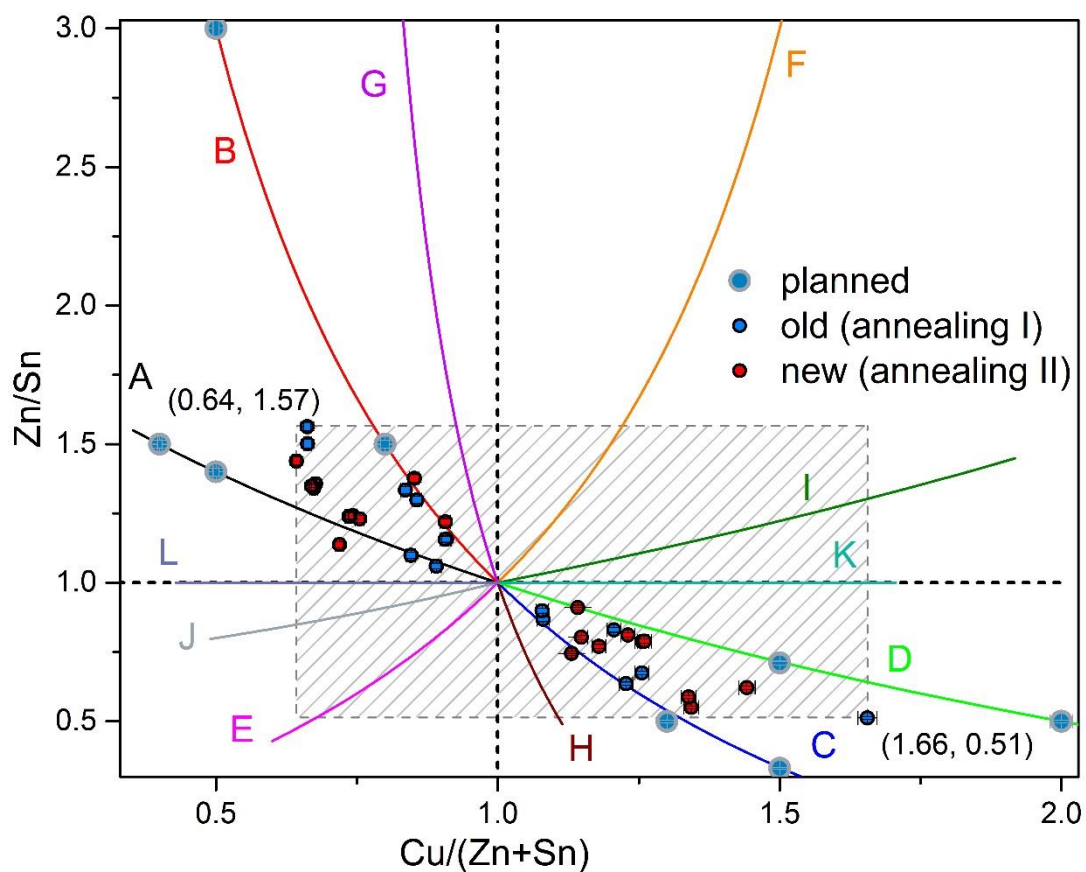
Table 1. The intended cation ratios Cu/(Zn+Sn) and Zn/Sn of the 8 far off-stoichiometric samples

Type	Sample name	Cu/(Zn+Sn)	Zn/Sn
A	A-001	0.5	1.4
	A-002	0.4	1.5
B	B-001	0.8	1.5
	B-002	0.5	3
C	C-001	1.33	0.5
	C-002	1.5	0.333
D	D-001	1.5	0.714
	D-002	2	0.5

Table 2. Overview of quarternary phases of the synthesized CZTSe samples: cation ratios Cu/(Zn + Sn) and Zn/Sn obtained from the electron microprobe analysis, occurring secondary phases and the off-stoichiometry types are given.

sample		formula	Cu/(Zn+Sn)	Zn/Sn	type	secondary phases
A-001	old	$Cu_{1.52}Zn_{1.42}Sn_{0.91}Se_4$	0.66	1.56	B - A	SnSe$_2$; ZnSe
		$Cu_{1.85}Zn_{1.06}Sn_{1.01}Se_4$	0.89	1.06	L - A	
	new	$Cu_{1.62}Zn_{1.22}Sn_{0.73}Se_4$	0.74	1.24	B - A	SnSe$_2$; ZnSe
		$Cu_{1.51}Zn_{1.30}Sn_{0.62}Se_4$	0.67	1.34	B - A	
		$Cu_{1.57}Zn_{1.16}Sn_{1.03}Se_4$	0.72	1.14	L - A	
A-002	old	$Cu_{1.51}Zn_{1.39}Sn_{0.93}Se_4$	0.66	1.50	B - A	SnSe$_2$; ZnSe
		$Cu_{1.78}Zn_{1.10}Sn_{1.00}Se_4$	0.85	1.10	L - A	
	new	$Cu_{1.52}Zn_{1.31}Sn_{0.96}Se_4$	0.68	1.36	B - A	SnSe$_2$; ZnSe; Zn
		$Cu_{1.47}Zn_{1.37}Sn_{0.95}Se_4$	0.64	1.44	B - A	
		$Cu_{1.57}Zn_{1.22}Sn_{0.98}Se_4$	0.74	1.24	B - A	
B-001	Old	$Cu_{1.84}Zn_{1.21}Sn_{0.93}Se_4$	0.86	1.30	B - A	ZnSe
		$Cu_{1.89}Zn_{1.12}Sn_{0.97}Se_4$	0.91	1.16	B - A	
	new	$Cu_{1.91}Zn_{1.15}Sn_{0.95}Se_4$	0.91	1.22	B - G	ZnSe
		$Cu_{1.85}Zn_{1.25}Sn_{0.91}Se_4$	0.85	1.38	B - G	
		$Cu_{1.65}Zn_{1.21}Sn_{0.98}Se_4$	0.75	1.22	B - A	
B-002	old	$Cu_{1.89}Zn_{1.12}Sn_{0.97}Se_4$	0.91	1.16	B - A	ZnSe
		$Cu_{1.81}Zn_{1.24}Sn_{0.93}Se_4$	0.84	1.33	B - A	
	new	$Cu_{1.62}Zn_{1.22}Sn_{0.98}Se_4$	0.74	1.24	B - A	ZnSe
		$Cu_{1.51}Zn_{1.31}Sn_{0.97}Se_4$	0.67	1.35	B - A	
		$Cu_{1.57}Zn_{1.16}Sn_{1.02}Se_4$	0.72	1.14	L - A	
C-001	old	$Cu_{2.20}Zn_{0.70}Sn_{1.1}Se_4$	1.23	0.64	C - D	SnSe$_2$; Cu$_2$SnSe$_3$
		$Cu_{2.08}Zn_{0.90}Sn_{1.03}Se_4$	1.08	0.87	C - D	
	new	$Cu_{2.19}Zn_{0.81}Sn_{1.05}Se_4$	1.18	0.77	C - D	SnSe$_2$; Cu$_2$SnSe$_3$
		$Cu_{2.31}Zn_{0.61}Sn_{1.12}Se_4$	1.34	0.55	C - D	
C-002	old	$Cu_{2.70}Zn_{0.24}Sn_{1.20}Se_4$	1.91	0.20	C - D	Cu$_2$SnSe$_3$; Cu$_2$Se
		$Cu_{2.29}Zn_{0.80}Sn_{1.02}Se_4$	1.26	0.79	C - D	
	new	$Cu_{2.16}Zn_{0.84}Sn_{1.04}Se_4$	1.15	0.80	C - D	Cu$_2$SnSe$_3$; Cu$_2$Se; SnSe$_2$
		$Cu_{2.32}Zn_{0.64}Sn_{1.10}Se_4$	1.34	0.59	C - D	
D-001	old	$Cu_{2.64}Zn_{0.55}Sn_{1.07}Se_4$	1.66	0.51	C - D	Cu$_2$Se
		$Cu_{2.24}Zn_{0.84}Sn_{1.02}Se_4$	1.21	0.83	C - D	
	new	$Cu_{2.30}Zn_{0.81}Sn_{1.02}Se_4$	1.26	0.79	C - D	Cu$_2$Se
		$Cu_{2.18}Zn_{0.91}Sn_{1.00}Se_4$	1.14	0.91	C - D	
D-002	old	$Cu_{2.25}Zn_{0.72}Sn_{1.07}Se_4$	1.26	0.67	C - D	Cu$_2$SnSe$_3$; SnSe$_2$
		$Cu_{2.09}Zn_{0.92}Sn_{1.02}Se_4$	1.08	0.90	C - D	
	new	$Cu_{2.45}Zn_{0.66}Sn_{1.06}Se_4$	1.44	0.62	C - D	Cu$_2$SnSe$_3$; Cu$_2$Se
		$Cu_{2.27}Zn_{0.83}Sn_{1.02}Se_4$	1.23	0.81	C - D	